

Tabla 3. Parámetros para el método LA.

I	$A_0$	$A_1$	$B_0$	$B_1$	$\Delta/mV$
0.5	0.017559	0.021798	-0.065646	0.021798	0.03
1	-0.031895	0.004057	-0.055682	0.004057	0.02
2	-0.058833	0.006262	-0.026422	0.006262	0.06
3	-0.082952	0.003776	-0.019672	0.003776	0.07
4	-0.097464	0.000377	-0.008274	0.000377	0.07

$g_1 = 0$  ( $A_1 = B_1$ );  $n/n_T = 0/25$ ;  $\sigma = 0.04$  mV.

I	$A_0$	$A_1$	$B_0$	$B_1$	$\Delta/mV$
0.5	0.017559	0.021798	-0.065746	0.022413	0.03
1	-0.031895	0.004057	-0.055887	0.004671	0.02
2	-0.058833	0.006262	-0.026832	0.006877	0.06
3	-0.082952	0.003776	-0.020286	0.004390	0.07
4	-0.097464	0.000377	-0.009094	0.000992	0.07

$g_1 = 0.000205$ ;  $n/n_T = 0/25$ ;  $\sigma = 0.06$  mV.

parámetros correspondientes a los dos electrolitos, a partir de los datos experimentales del primero de ellos.

#### REFERENCIAS

- 1.- Lim, T.K., *Int. J. Quantum Chem.* 16, 247 (1982).
- 2.- Lim, T.K.; Chan, C.Y. y Khoo, K.H., *J. Solution Chem* 9, 507 (1980).
- 3.- Friedman, H.L. en *Ionic Solution Theory* (Interscience, N.Y., 1962).
- 4.- Lim, T.K., *J. Chem. Soc Faraday Trans I*, 82, 69 (1986).
- 5.- Esteso, M.A.; Fernández Mérida, L.; Hernández Luis, F. y González Díaz, O., *Ber. Bunsenges. Phys. Chem.* 93, 213 (1989).
- 6.- Fernández Mérida, L. y Hernández Luis, F., resultados no publicados.
- 7.- Pitzer, K.S. y Kim, J.J., *J. Am. Chem. Soc.* 96, 5701 (1974).
- 8.- Pitzer, K.S., *J. Solution Chem.* 4, 249 (1975).
- 9.- Lim, T.K., *J. Solution Chem.* 16, 917 (1987).

#### THE PHOTOCHEMISTRY OF 1-IODOANTHRAQUINONE RADICAL ANION

Richard G. Compton, Adrian C. Fisher, R. Geoffrey Wellington and †Donald Bethell.  
Physical Chemistry Laboratory, Oxford University, OXFORD OX1 3QZ.

†Department of Chemistry, Liverpool University, P.O.Box 147, LIVERPOOL L69 3BX.

#### ABSTRACT

The photochemical reaction of 1-iodoanthraquinone under electrochemical reduction in acetonitrile with tetrabutylammonium perchlorate as supporting electrolyte, is investigated. Irradiation with light corresponding to an absorption band of the 1-iodoanthraquinone radical anion, is shown to produce the radical anion of anthraquinone via a mixed ECE/DISP1 mechanism. The rate of iodide anion expulsion is quantified: excitation at 565 nm is approximately 7.5 times faster than excitation at 417 nm.

#### INTRODUCTION

We have shown previously<sup>1</sup> how channel electrode methodology can be employed to study photoelectrochemical processes. Using this approach we investigate here the light-induced iodide expulsion from the electro-generated radical anion of 1-iodoanthraquinone (AQI). The efficiency of this process is investigated at two different absorption wavelengths.

#### EXPERIMENTAL

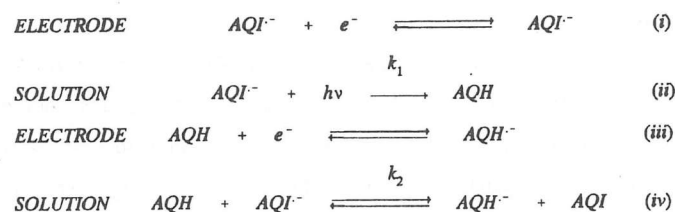
Electrochemical, photoelectrochemical and in-situ ESR experiments employed a channel electrode of standard construction and dimensions<sup>1</sup>, with a gold working electrode. Experiments were performed using solutions of AQI (ca 10<sup>-3</sup>M) in dried acetonitrile solution containing 0.1M tetrabutylammonium perchlorate (TBAP) as supporting electrolyte. Solutions were purged of oxygen by outgassing with prepurified nitrogen prior to electrolysis. AQI was prepared according to the method of Goldstein<sup>2</sup>.

#### RESULTS AND DISCUSSION

The 'dark' electrochemical behaviour of AQH and AQI was investigated initially in the medium specified, showing, in each case, one electron reversible reductions to the corresponding radical anions AQH<sup>-</sup> ( $E^0 = 0.900$  V) and AQI<sup>-</sup> ( $E^0 = 0.826$  V). In-situ

channel electrode/ESR experiments showed that reduction at the potentials cited above led to strong ESR signals. In both cases spectra obtained were identical to those reported for, AQH<sup>-3</sup> and AQI<sup>-4</sup>. The UV/visible spectrum of AQI<sup>-</sup> measured using an OTTLE<sup>1</sup> showed absorption bands centred on 565nm and 417nm. These bands had extinction coefficients in the ratio  $\epsilon_{417}/\epsilon_{565} = 0.50 \pm 0.06$  and a value of  $7.0 \times 10^3 \text{ dm}^3 \text{ mol}^{-1} \text{ cm}^{-1}$  was estimated for  $\epsilon_{565}$ . The parent AQI shows negligible absorption above 400nm<sup>1</sup>.

Photoelectrochemical experiments used a channel flow cell located in the cavity of an ESR spectrometer. A solution of AQI was flowed through the cell, reduced electrolytically to AQI<sup>-</sup> and the ESR spectrum of the latter recorded. The cell was then irradiated (417nm or 565nm) inside the cavity. Strong ESR signals corresponding to AQH<sup>-</sup> were observed along with substantial photocurrents. The photo-induced expulsion of iodide from AQI<sup>-</sup> was inferred. The precise mechanism of this process was deduced with measurements of dark currents and photo-currents recorded over a wide range of flow rates ( $V_f$ ) and different light intensities,  $I$ , (0-40mWcm<sup>-2</sup>). The electrode was held at a potential corresponding to the transport limited reduction of AQI and AQH. The 'effective' number of electrons transferred in the photo-reaction,  $N_{\text{eff}}$ , was calculated for each flow rate by dividing the photocurrent by the dark current.  $N_{\text{eff}}$  was found to vary such that  $1 < N_{\text{eff}} < 2$ , consistent with the transformation of AQI into AQH<sup>-</sup>. Also  $N_{\text{eff}} \rightarrow 2$  as  $V_f \rightarrow 0$  or  $I \rightarrow \infty$ ; this is suggestive<sup>5</sup> of an ECE/DISP process. The following mechanistic scheme is proposed:



The basis for the resolution of these various possibilities via the flow rate dependence of  $N_{\text{eff}}$  has been presented elsewhere<sup>5</sup>. For mechanisms where the first-order reaction (ii) is rate-determining, a normalised rate constant<sup>5</sup>,  $K_1 \propto k_1 V_f^{-2/3}$  is employed and values are deduced from  $N_{\text{eff}}$  via a 'working curve'<sup>5</sup>. If the deduced values of  $K_1$  are plotted against  $V_f^{-2/3}$  a straight line through the origin will result, but only in the case of the correct mechanism having been selected: this is the basis of the required mechanistic

discrimination. The photocurrent data obtained at 565nm when analysed exhibited a mixed ECE/DISP1 mechanism. Modelling was performed for different values of the rate constant,  $k_2$ , for reaction (iv) in the forward direction. The rate constant for the reverse direction was deduced from  $k_2$  since these are related through the equilibrium constant,  $K^*$ , for reaction (iv) and this is readily deduced from the formal potentials for the AQH/AQH<sup>-</sup> and AQI/AQI<sup>-</sup> redox couples, ( $K^* = 0.056$ ). The best fit was obtained when  $k_2 = 10^8 \text{ cm}^3 \text{ mol}^{-1} \text{ s}^{-1}$ . Figure 1 shows this analysis, for five separate light intensities. Knowledge of the cell geometry gave the rate constant  $k_1 = 1.91 \text{ s}^{-1}$  ( $I = 39.9 \text{ mWcm}^{-2}$ ) (figure 1).

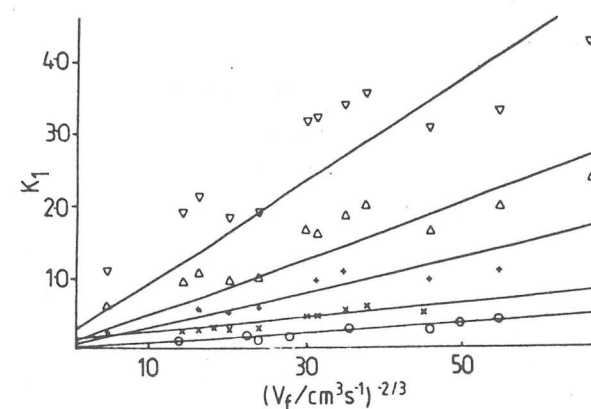


Figure 1 Analysis of photocurrent measurements from excitation of AQI<sup>-</sup> at 565nm for light intensities (o) 1.7, (x) 3.7 (+) 8.2 (Δ) 18.0 and (▽) 39.9 mWcm<sup>-2</sup>.

Next photocurrent/flow rate experiments were performed using light of wavelength 417nm corresponding to a different absorption band of AQI<sup>-</sup>. The procedure was identical to that used at 565nm and values of dark current and photocurrent gave  $N_{\text{eff}}$  for each flow rate and different light intensities. These were analysed using the working curve as before, keeping the parameters  $k_2 = 10^8 \text{ cm}^3 \text{ mol}^{-1} \text{ s}^{-1}$  and  $K^* = 0.056$ .  $K_1$  was deduced from the experimental values of  $N_{\text{eff}}$  and plotted against  $V_f^{-2/3}$ . The resulting straight lines are shown in figure 2 and show the ECE/DISP1 mechanism to be again appropriate. It may be concluded that the mixed ECE/DISP1 mechanism is operating at both wavelengths studied, but the kinetics are much slower at 417nm.

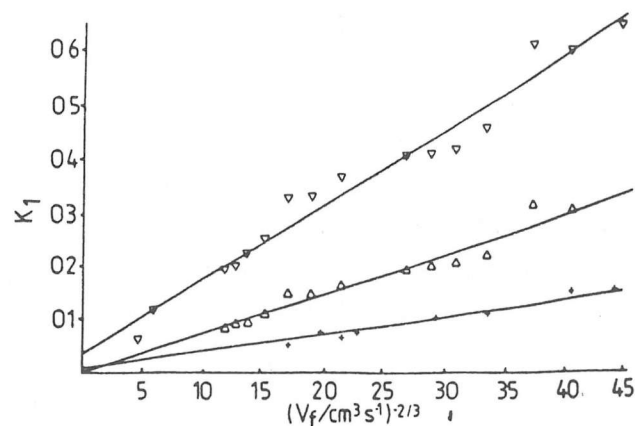


Figure 2 Analysis of photocurrent measurements from excitation of AQI at 417nm for light intensities (o) 1.7, (x) 3.7 (+) 8.2 (∆) 18.0 and (∇) 39.9 mWcm<sup>-2</sup>.

On the basis of the extinction coefficients cited above it can be seen that the rate of iodide expulsion is 7.4 ( $\pm 0.9$ ) times lower per photon absorbed at 417 nm than at 565 nm.

#### CONCLUSION

Channel electrode studies have shown that the photo-reduction of AQI proceeds via a mixed ECE/DISP1 mechanism and the kinetics of iodide expulsion has been quantified. It has been found that the different excited states of the AQI radical anion, obtained through excitation at either 417 or 565nm, show different dynamic behaviour. In particular expulsion is some 7.4 times faster per photon absorbed with 565nm radiation than with 417nm. Further work, quantifying excited state lifetimes and spin densities, will seek to explain this behaviour.

#### REFERENCES

- 1) R.G.Compton, B.A.Coles, M.B.G.Pilkington and D.Bethell, *J.Chem.Soc., Faraday Trans.*, 663,86,(1990).
- 2) A.E.Goldstein, *J.Am.Chem.Soc.*, 1600,61,(1939).
- 3) H.Gerischer, I.Mattes and R.Brown, *J.Electroanal.Chem.*, 553,10,(1965).
- 4) M.Adams, M.S.Blois and R.H.Sands, *J.Chem.Phys.*, 774,28,(1958).
- 5) C.Amatore and J.M.Saveant, *J.Electroanal.Chem.*, 27,85,(1981).

#### APPLICATION OF IN-SITU SNIFTIRS TO THE STUDY OF THE ELECTROREDUCTION OF DIOXYGEN ON GOLD

P. Christensen\*, C. Paliteiro# and A. Hamnett\*

(\* Department of Chemistry, University of Newcastle, England

(# Department of Chemistry, University of Coimbra, Portugal

This communication reports preliminary results obtained in a study of the electroreduction of dioxygen on different electrode materials applying in-situ SNIFTIRS. With this study we hope to be able to characterize the material surface in the absence of O<sub>2</sub> and to detect and characterize intermediates of the electroreduction reaction. We started by examining O<sub>2</sub> reduction on gold in alkaline solutions. In our experiments we used a thin layer cell with a CaF<sub>2</sub> window and a 7 mm diameter, 3 mm thick Au disc mounted in a teflon body. Saturated calomel and Hg/HgO electrodes were used as reference electrodes, but hereafter potentials are referred to RHE, the reversible hydrogen electrode (0 V/SCE = 1.06 V/RHE and 0 V/Hg/HgO = 0.94 V/RHE). Spectra were collected using a Biorad FTS-40 spectrometer interfaced to a 6800-based microcomputer supplied by OxyS Micros. In the following figures the ordinate represents the reflectance measured at a given potential and wavenumber relatively to the reflectance measured at a reference potential and the same wavenumber. Features pointing up, i.e. to relative reflectance > 1, correspond to a loss of the starting material, whereas features going down, i.e. to relative reflectance < 1, correspond to gain of a product.

Two types of experiments were carried on:

a) In one of them the reference spectrum was taken at 1.11 V (chosen as the potential where O<sub>2</sub> is not reduced); then the potential was stepped to successively more cathodic values and further spectra were collected. These spectra are shown in Fig 1 ratioed to the reference spectrum.

The spectra show two main loss features at  $\approx 1660$  and  $\approx 3150$  cm<sup>-1</sup> and one main gain feature at  $\approx 3800$  cm<sup>-1</sup>. We assign these two loss features to the loss of adsorbed water from the electrode surface; therefore the bands at 1660 and 3150 cm<sup>-1</sup> correspond respectively to the bending mode and to the O-H stretching mode of H<sub>2</sub>O. The low frequency of this last band and its large width are characteristic of hydrogen-bonded water [1]; the shoulder at  $\approx 3580$  cm<sup>-1</sup> may be due